Cell Host & Microbe, Volume *21*

Supplemental Information

Betacoronavirus Adaptation to Humans Involved Progressive Loss of Hemagglutinin-Esterase Lectin Activity

Mark J.G. Bakkers, Yifei Lang, Louris J. Feitsma, Ruben J.G. Hulswit, Stefanie A.H. de Poot, Arno L.W. van Vliet, Irina Margine, Jolanda D.F. de Groot-Mijnes, Frank J.M. van Kuppeveld, Martijn A. Langereis, Eric G. Huizinga, and Raoul J. de Groot

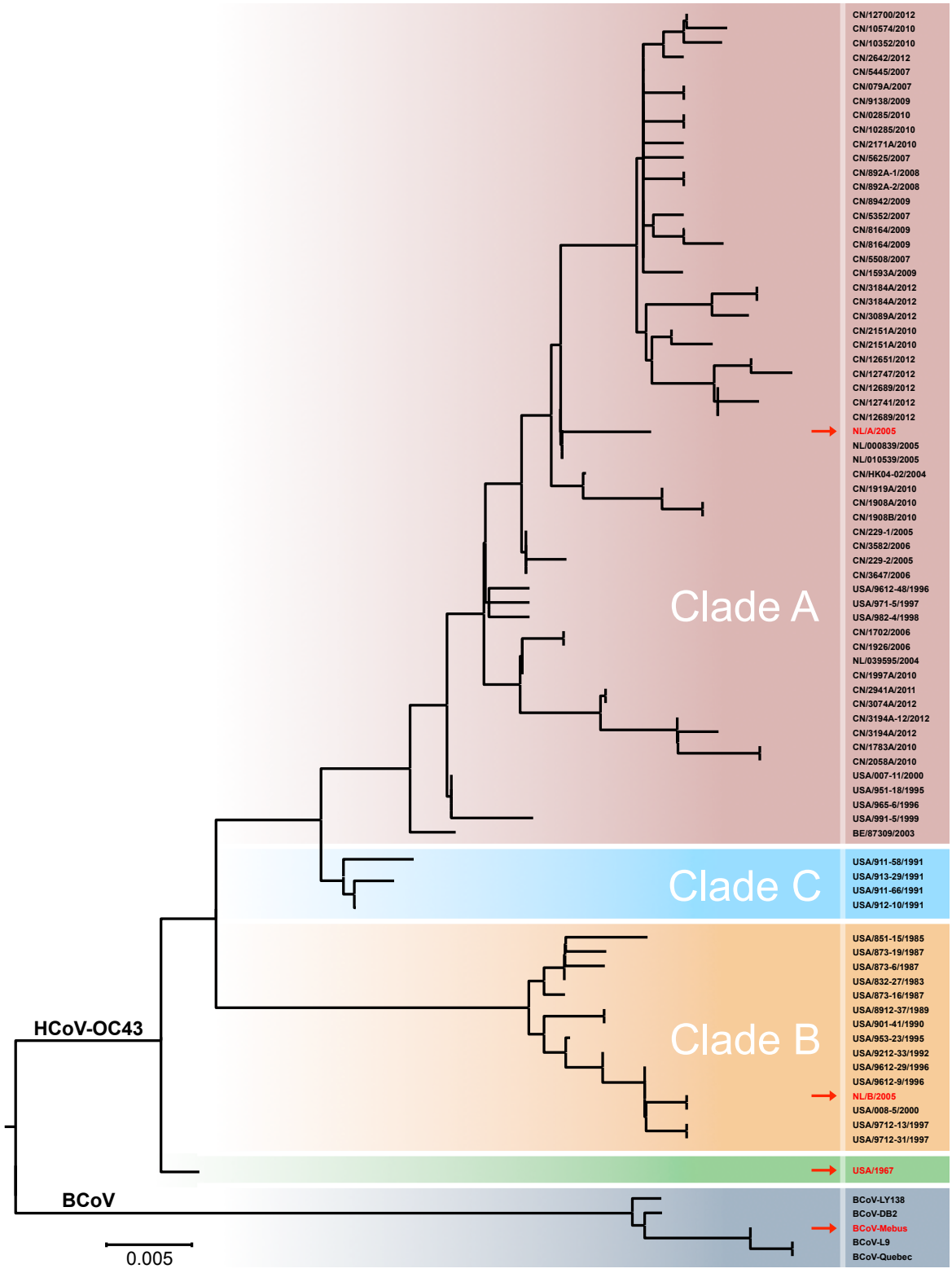

sFigure 1. Neighbor-Joining phylogenetic tree based on all OC43 HE sequences in the NCBI database, *related to Figure 1*. Evolutionary distances were computed using the Maximum Composite Likelihood method in MEGA6. BCoV HEs were included as an outgroup. OC43 HE sequences of unknown sampling date were omitted from the final tree. The different clades are color-coded with OC43 USA/1967 in green, and OC43 clades A-C in purple, orange and blue, respectively. A number of representative BCoV HEs are shaded in dark blue. HEs used in this study are shown in red and indicated with a red arrow.

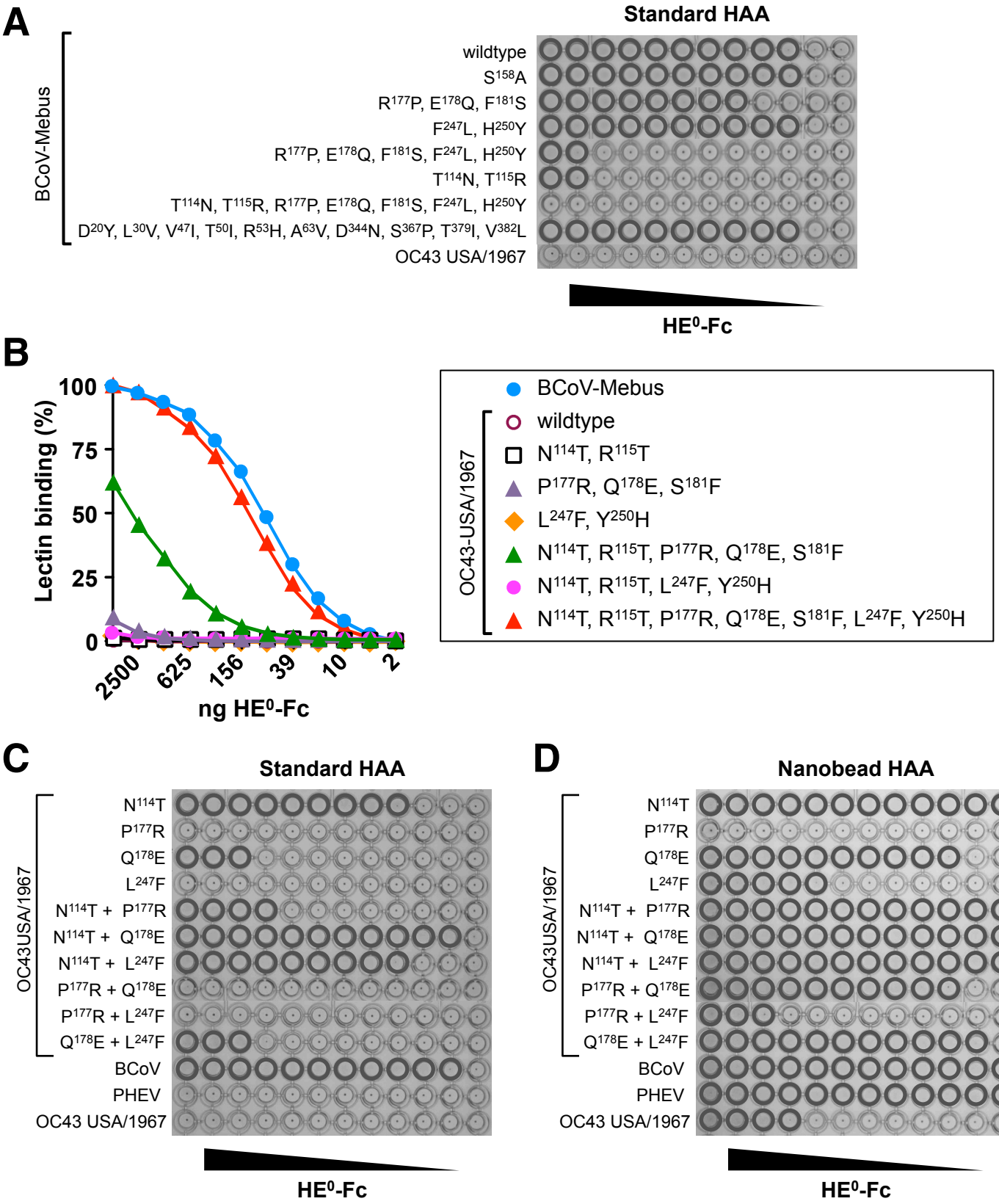

sFigure 2. Lectin affinity prescreen of OC43 USA/1967 HE specific mutations, *related to Figure 2*. (A) Mutations of OC43 USA/1967 HE were placed in the background of BCoV-Mebus HE^0 in sets and tested in standard HAA. (B) Corresponding residues from BCoV-Mebus HE were placed in the background of OC43 USA/1967 HE^0 in sets and tested by sp-LBA. (C, D) Single and double mutations from BCoV-Mebus HE were placed in the background of OC43 USA/1967 HE^0 and tested by standard HAA (C) and by nanobead HAA (D).

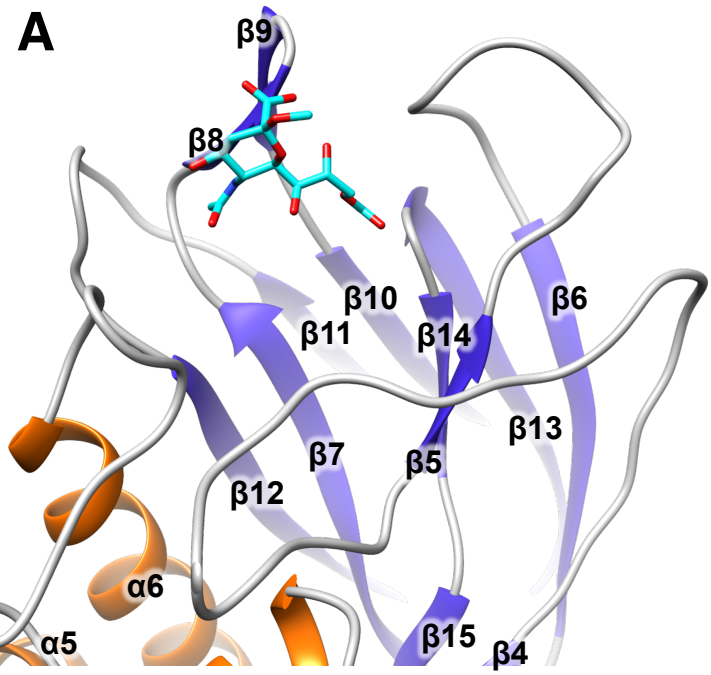

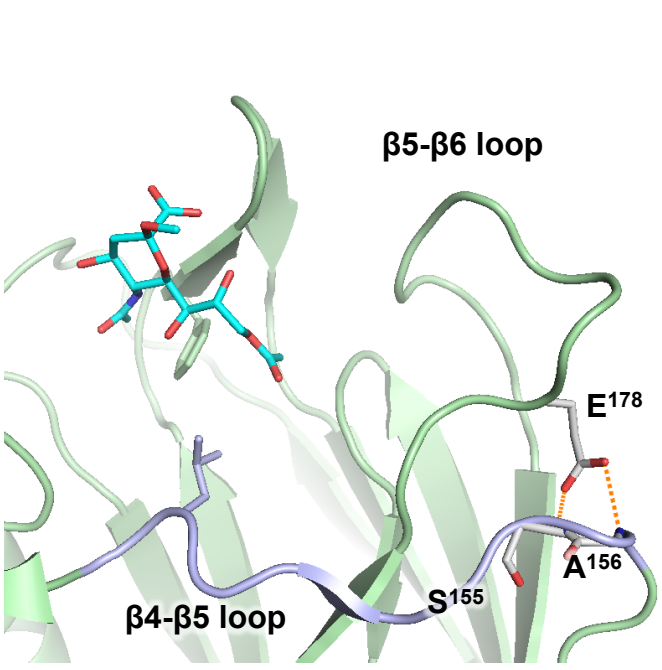

C

OC43 USA/1967 GGGGATTATTATTATAAG
G D Y Y Y K

OC43 NL/A/2005 GGG-ATTATTAC--TAAG
G I I T K

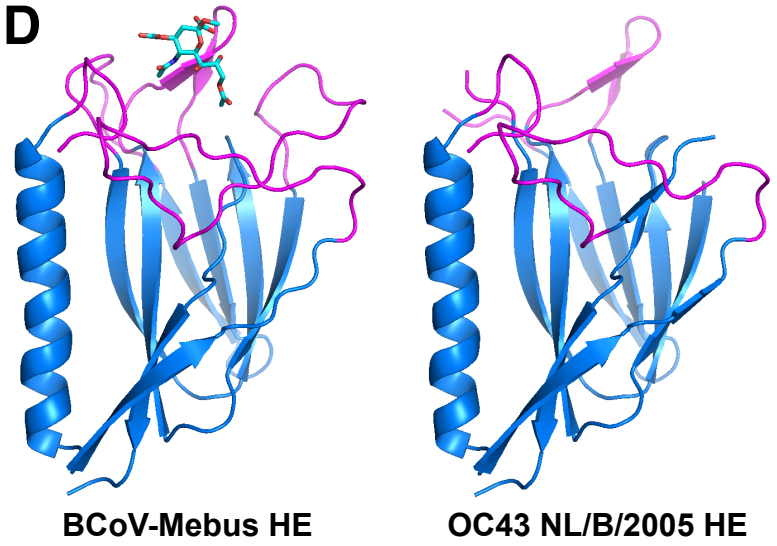

sFigure 3. Structural and sequence comparison of BCoV and OC43 HE, *related to Figure 2*. (A) Cartoon representation of the lectin domain of BCoV-Mebus HE in complex with 9-*O*-Ac-Sia (PDB ID: 3CL5). The structure is colored according to secondary structure with α-helices in orange and β-strands in blue. The receptor analogue in stick representation is colored according to atom type with carbon in cyan, oxygen in red and nitrogen in blue. Secondary structure elements are numbered sequentially. (B) E^{178} indicated in a cartoon representation of the lectin domain of BCoV-Mebus HE in complex with 9-*O*-Ac-Sia. E^{178} is located in the β5-β6 loop from where it can form hydrogen bonds with S^{155} and A^{156} present in the β4-β5 loop (shown in purple). The receptor analogue in stick representation is colored as in sFig. 3. (C) A presumptive frameshift mutation in OC43 NL/A/2005 HE. Coding sequence of the DYYY to IIT mutation, with codons underlined alternatingly in black and red. Conserved bases are in blue, and mutations/deleted bases are in red. (D) Comparison of the overall fold of the lectin domains of BCoV-Mebus HE in complex with 9-*O*-Ac-Sia and of OC43 NL/A/2005 HE. Structures are shown as cartoons with the structurally conserved scaffold in blue and the extended loops that form the receptor binding site in pink. The receptor analogue is shown as in A.

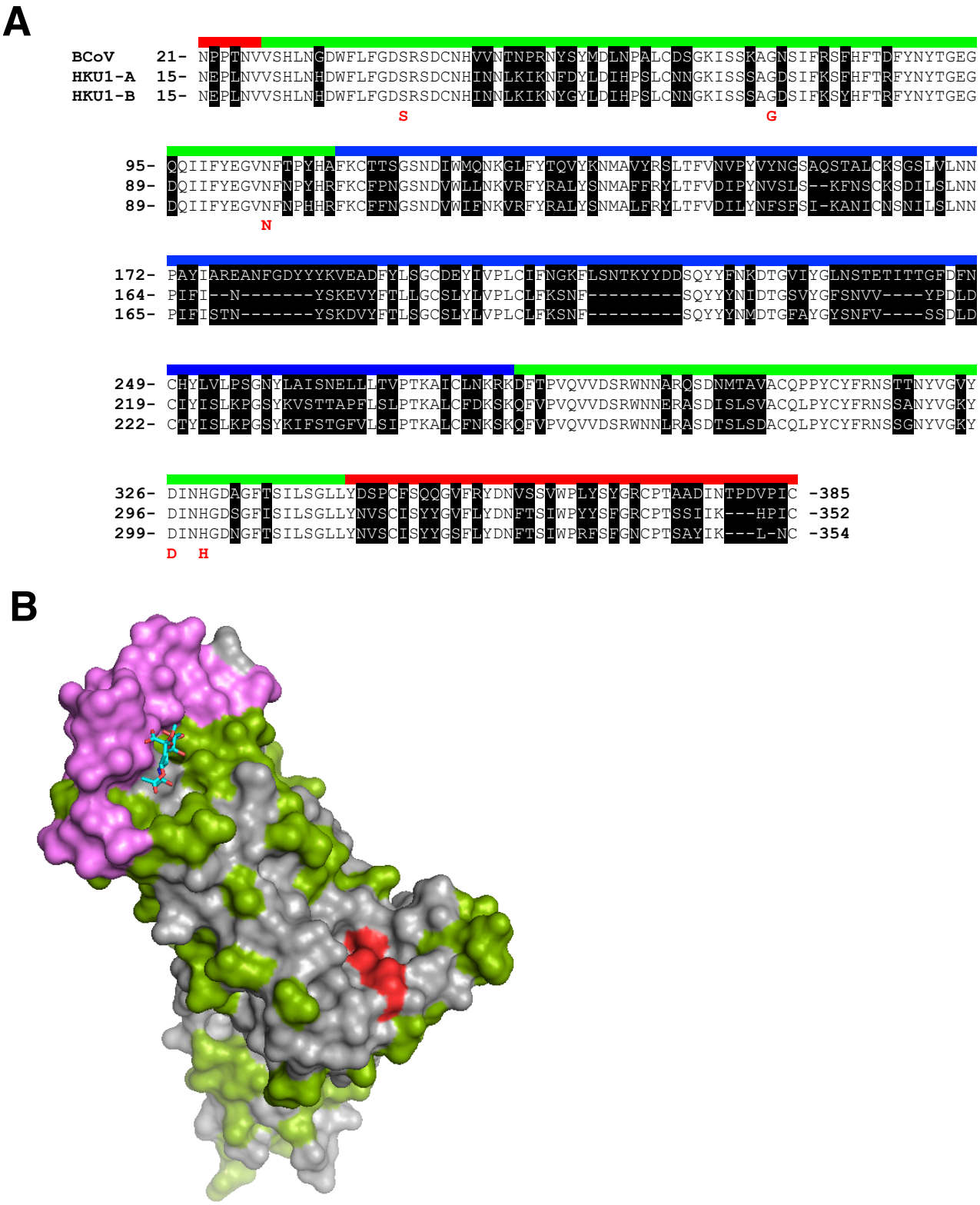

sFigure 4. Comparison of BCoV HE and HKU1 HE, *related to Figure 5.* (A) Amino acid alignment of BCoV HE with representatives of the two HCoV-HKU1 HE clades (designated clades A and B). Domain organization is color-coded (membrane-proximal domain, red; esterase domain, green; lectin domain, blue). Residues crucial for esterase activity (SGNDH) are annotated below. Amino acid differences are marked in black. (B) Surface representation of BCoV-Mebus HE in complex with 9-*O*-Ac-Sia (PDB ID: 3CL5) with the amino acid mutations (green) and deletions (violet) that occurred in HKU1 HE visualized. The catalytic triad is indicated in red.

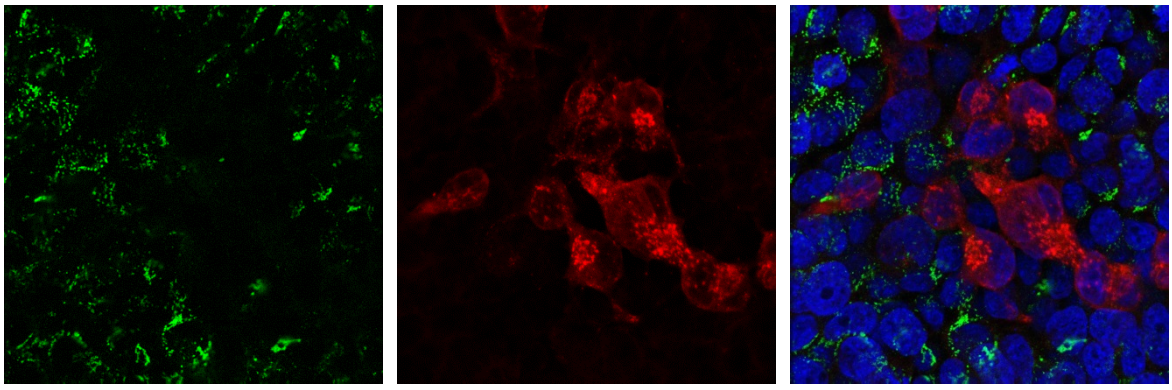

sFigure 5. Destruction of endogenous receptors in OC43-infected HEK293T cells, *related to Figures 5 and 6*. Cells were PFA-fixed, Triton-X100-permeabilized and double-stained for 9-*O*-Ac-Sia with virolectin P4 (Langereis et al., 2015) and for OC43 proteins with serum from a BCoV-infected cow. Nuclei (N) stained with Hoechst-33258.

sTable 1. Data collection and refinement statistics *(Related to Figure 4)*

	HCoV-OC43 NL/A/2005 HE*
Data Collection	
Wavelength (Å)	1.0000
Space group	$P3_221$
Cell dimensions a, b, c (Å) α, β, γ (°)	 77.73, 77.73, 299.49 90, 90, 120
Resolution range (Å)**	74.9 - 2.45 (2.55 – 2.45)
Total no. reflections	236791 (23722)
No. unique reflections	39833 (4378)
R_{merge}	0.093 (0.377)
I/σI	10.9 (3.8)
Redundancy	5.9 (5.4)
Completeness (%)	99.3 (98.8)
CC(1/2)	0.997 (0.586)
Refinement	
R_{work} / R_{free}	0.2115 / 0.2501
No. atoms	
Protein	5483
Water / other ligands	49 / 538
Average B / Wilson B ($Å^2$)	24.2 / 46.5
RMS deviations	
Bond lengths (Å)	0.0054
Bond angles (°)	1.1181
Ramachandran Plot	
Favored (%)	94.1
Allowed (%)	5.4
Outliers (%)	0.4

* PDB ID: 5N11

**Numbers between brackets refer to the outer resolution shell.

sTable 2. Comparative numbers of virus particles in purified preparations of HCoV-OC43 and BCoV as determined by quantitative EM and plaque assay (each for equivalents of 15 mU esterase) and by semiquantitative real-time RT-PCR (relative genome content). All measurements are based on independent experiments performed at least in triplicate. *(Related to Figure 6)*

	Esterase units	**Particles**	**PFU**	**Genome content (ratio)**
HCoV-OC43 USA/1967	15 mU	$0.44\pm0.07*10^{10}$	$1.21\pm0.08*10^{7}$	1 ± 0.13
BCoV Mebus	15 mU	$1.16\pm0.09*10^{10}$	$3.04\pm0.11*10^{7}$	2.9 ± 0.22

Supplemental Experimental Procedures

pNPA assay. HE esterase activity towards 4-nitrophenyl acetate (pNPA) was determined by detection of the chromogenic p-nitrophenolate anion (pNP) that is formed upon hydrolysis (Vlasak et al., 1987). Briefly, 50 ng HE was incubated with 1 mM pNPA in PBS and the amount of pNP was determined spectrophotometrically at 405 nm every 20 sec for 15 min. Assays were corrected for spontaneous hydrolysis of pNPA. One unit was defined as the amount of enzymatic activity resulting in the cleavage of 1 µmol of *p*NPA per min. The specific activities of the varies HE^+-Fc proteins were expressed in mU/µg of protein and shown in graphs as percentages of wildtype BCoV HE^+-Fc activity.

Cells and viruses. Cells were maintained in Dulbecco's modified Eagle's medium (DMEM, Lonza) supplemented with 10 % heat-inactivated fetal calf serum (FCS), penicillin (100 IU/ml), and streptomycin (100 µg/ml). Recombinant MHV-A59 (rMuCoV) derivatives with the autologous gene for HE replaced by that of BCoV-Mebus or OC43 USA/1967 were constructed by targeted RNA recombination (Kuo et al., 2000) and propagated in LR7 cells (Lissenberg et al., 2005). BCoV strain Mebus and OC43 strain USA/1967, obtained from the American Type Culture Collection, were propagated in HRT-18 cells.

Purification of virions for whole virus receptor-destruction assays. Concentrated stocks of purified viruses were prepared by inoculating cell monolayers at an MOI of 0.01 PFU/cell for 1 hr. Virus-containing cell culture supernatants (Opti-MEM; Gibco), harvested at 18 hr (rMuCoVs) or 72 hr after infection (BCoV-Mebus and OC43 USA/1967), were clarified by consecutive centrifugation at 1200rpm, 4°C for 5 min and at 4000 rpm, 4°C for 10 min. Virions were purified and concentrated by their centrifugation through 20% (w/v) sucrose cushions (80,000g, 2 hr, 4°C), and resuspended in PBS. Aliquots were stored at -80°C. BCoV and OC43 preparations were assessed for particle content by qPCR (SYBR Green real-time PCR (Life Technologies) using primers 5'-TGCAAATTACGCGGCAAG-3' and 5'-AACCAATGCCAGCAACACTAGC-3', plaque assay in HRT18 cells, quantitative latex bead ratio electron microscopy (EM) , and by pNPA esterase activity assay.

Crystallization and X-ray data collection. OC43 NL/A/2005 HE crystals with $P3_221$ spacegroup were grown at 20°C using sitting drop vapor diffusion against a well solution containing 0.2M NaCl, 10mM KCl, 0.1M NaAc pH 5.0 and 20% PEG6000 (w/v). Crystals were cryoprotected in well solution containing 20% (v/v) glycerol before flash-freezing in liquid nitrogen. Diffraction data to 2.45 Å resolution were collected at the Swiss Light Source (Villigen, Switzerland) on the PX beamline and integrated with Mosflm (Leslie and Powell, 2007). Integrated diffraction data were further processed using the CCP4 package (Winn et al., 2011). The structure was solved by molecular replacement using the BCoV-Mebus HE structure (PDB ID: 3CL5) as search model (Zeng et al., 2008). Models were refined using REFMAC (Vagin et al., 2004) alternated with manual model improvement using COOT (Emsley et al., 2010). Refinement procedures included TLS refinement using one TLS group for each of the HE monomers in the asymmetric unit. The resulting crystal structure had R_{work} and R_{free} final values of 21.2% and 25.0%. Statistics of data processing and refinement are listed in sTable 1.

Supplemental References

Emsley, P., Lohkamp, B., Scott, W.G., and Cowtan, K. (2010). Features and development of Coot. Acta Crystallogr. Sect. D Biol. Crystallogr. *66*, 486–501.

Kuo, L., Godeke, G., Raamsman, M.J.B., Masters, P.S., and Rottier, P.J.M. (2000). Retargeting of coronavirus by substitution of the spike glycoprotein ectodomain: crossing the host cell species barrier. J. Virol. *74*, 1393–1406.

Langereis, M.A., Bakkers, M.J.G., Deng, L., Padler-Karavani, V., Vervoort, S.J., Hulswit, R.J.G., van Vliet, A.L.W., Gerwig, G.J., de Poot, S.A.H., Boot, W., et al. (2015). Complexity and diversity of the mammalian sialome revealed by nidovirus virolectins. Cell Rep. *11*, 1966–1978.

Leslie, A., and Powell, H. (2007). Evolving Methods for Macromolecular Crystallography. Evol Methods Macromol Crystallogr *245*, 41–51.

Lissenberg, A., Vrolijk, M., van Vliet, A.L.W., Langereis, M.A., Groot-Mijnes, J.D.F. de, Rottier, P.J.M., and de Groot, R.J. (2005). Luxury at a cost? Recombinant mouse hepatitis viruses expressing the accessory hemagglutinin esterase protein display reduced fitness in vitro. J. Virol. *79*, 15054–15063.

Vagin, A.A., Steiner, R.A., Lebedev, A.A., Potterton, L., McNicholas, S., Long, F., and Murshudov, G.N. (2004). REFMAC 5 dictionary: organization of prior chemical knowledge and guidelines for its use. Acta Crystallogr. Sect. D Biol. Crystallogr. *60*, 2184–2195.

Vlasak, R., Krystal, M., Nacht, M., and Palese, P. (1987). The influenza C virus glycoprotein (HE) exhibits receptor-binding (hemagglutinin) and receptor-destroying (esterase) activities. Virology *160*, 419–425.

Winn, M.D., Ballard, C.C., Cowtan, K.D., Dodson, E.J., Emsley, P., Evans, P.R., Keegan, R.M., Krissinel, E.B., Leslie, A.G.W., McCoy, A., et al. (2011). Overview of the CCP4 suite and current developments. Acta Crystallogr. D. Biol. Crystallogr. *67*, 235–242.

Zeng, Q., Langereis, M.A., van Vliet, A.L.W., Huizinga, E.G., and de Groot, R.J. (2008). Structure of coronavirus hemagglutinin-esterase offers insight into corona and influenza virus evolution. Proc. Natl. Acad. Sci. U. S. A. *105*, 9065–9069.